Anomalous temperature dependence of the superfluid density caused by a dirty-to-clean crossover in superconducting $FeSe_{0.4}Te_{0.6}$ single crystals

Hideyuki Takahashi,[1,3] Yoshinori Imai,[1,3] Seiki Komiya,[2,3] Ichiro Tsukada,[2,3] and Atsutaka Maeda[1,3]
[1]*Department of Basic Science, the University of Tokyo, 3-8-1 Komaba, Meguro-ku, Tokyo 153-8902, Japan*
[2]*Central Research Institute of Electric Power Industry, 2-6-1 Nagasaka, Yokosuka, Kanagawa 240-0196, Japan*
[3]*Transformative Research Project on Iron Pnictides (TRIP), JST, Japan*
(Received 2 August 2011; published 18 October 2011)

We report microwave surface impedances of $FeSe_{0.4}Te_{0.6}$ single crystals measured at 12, 19, and 44 GHz. The penetration depth exhibits a power-law behavior, $\delta\lambda_L = \lambda_L(T) - \lambda_L(0) \propto CT^n$ with an exponent $n \simeq 2$, which is considered to result from impurity scattering. The temperature dependence of the superfluid density largely deviates from the behavior expected in the BCS theory. We believe that this deviation is caused by the crossover from the dirty regime near T_c to the clean regime at low temperatures, which is supported by the rapid increase of the quasiparticle scattering time obtained from the microwave conductivity. We also believe that the previously published data of the superfluid density can be interpreted in this scenario.

DOI: 10.1103/PhysRevB.84.132503 PACS number(s): 74.25.nn, 74.20.Rp, 74.25.fc, 74.62.−c

Iron-based superconductors have attracted much attention since the discovery of $LaFeAsO_{1-x}F_x$ with $T_c = 28$ K.[1] These compounds are expected to have an unconventional pairing mechanism because they contain Fe, one of the most familiar ferromagnetic elements. Indeed, there have been many studies on various pairing symmetries of iron-based superconductors.[2–5] The penetration depth studies have also suggested that the details of the pairing symmetry depend on the materials.[6–9]

However, the estimates of the value of the superconducting gaps are inconsistent among different groups even in the same compounds.[2] One reason is that the temperature dependence of the superfluid densities $n_s(T)$ in some compounds cannot be understood in the framework of the BCS model. A typical example is $n_s(T)$ in $FeSe_{0.4}Te_{0.6}$, which we focus on in this Brief Report. $FeSe_{0.4}Te_{0.6}$[10] ($T_c = 14$ K) (the so-called 11 system) has the simplest crystal structure (PbO-type) among all iron-based superconductors. This compound does not contain arsenic, which is common in most iron-based superconductors, but the electronic structure of this system is similar to that of the FeAs layers.[11] It was suggested that $n_s(T)$ in $Fe_{1.03}Se_{0.37}Te_{0.63}$ can be fitted by a two gap model that takes into account interband scattering.[12] However, the model is based on the assumption that the sample is within the clean limit. In the 11 system, unlike ordinary metals, the resistivity of the material shows a small temperature dependence and has a relatively large value in the normal state: $\rho(15\ \mathrm{K}) \simeq 0.5$ mΩ cm.[13–15] Thus it is possible that there are unusual characteristics of quasiparticle scattering that affect the superconductivity and that produce some anomalous superconducting features. We believe that the microwave conductivity measurement is needed to evaluate the quasiparticle scattering in the superconducting state. In this Brief Report, we present the results of surface impedance measurements in $FeSe_{0.4}Te_{0.6}$ single crystals, from which we extracted the microwave conductivity σ and n_s. Then, we show that the crossover from the dirty regime near T_c to the clean regime at low temperatures can affect $n_s(T)$. We believe that the scenario is applicable to many other iron-based superconductors that have the "dirty" nature in the normal state.

The single crystals with nominal composition $FeSe_{0.4}Te_{0.6}$ were grown by the Bridgman method with annealing.[13–15] Composition analysis by the energy dispersive x-ray (EDX) method revealed that the actual Se/Te ratio is approximately Se : Te = 1 : 2. Although we could not know the exact amount of excess irons, since EDX analysis has an error of several percent, we did not observe significant Fe nonstoichiometry. We estimate excess iron in our samples is 3% at most, because our samples showed similar transport properties to the good superconducting sample in Ref. 16. The transition temperature determined from dc magnetic susceptibility is $T_c = 14$ K with the width $\Delta T < 0.5$ K, which is rather sharp.

The surface impedance $Z_s = R_s - iX_s$, where R_s is the surface resistance and X_s is the surface reactance, was measured by a cavity perturbation technique. We used three kinds of cylindrical oxygen-free Cu cavity resonators, operated in the TE_{011} mode at 12, 19, and 44 GHz, which have a quality factor, $Q \sim 60\,000$ (12 GHz, 19 GHz), and 26 000 (44 GHz), respectively. A piece of crystal is mounted on a sapphire rod and is placed in the antinode of the microwave magnetic field H_ω. H_ω is parallel to the c axis, so that the shielding current flows in the ab planes. In this technique, one measures the changes of Q and the resonant frequency f of the cavity, which are caused by introducing a sufficiently small sample. The shifts in the inverse of Q and f are proportional to R_s and X_s, respectively. The absolute values of Z_s were obtained by assuming the Hagen-Rubens limit ($\omega\tau \ll 1$), where $R_s = X_s = (\mu_0\omega\rho/2)^{\frac{1}{2}}$ above T_c ($\omega = 2\pi f$ is the angular frequency, τ is the quasiparticle scattering time, and μ_0 is the permeability in vacuum).

For the case of local electrodynamics, we can extract σ from Z_s using the relation $Z_s = (-i\mu_0\omega/\sigma)^{\frac{1}{2}}$. In the two-fluid model, σ is expressed as

$$\sigma = \sigma_1 + i\sigma_2 = \frac{n_n e^2 \tau}{m^*} \frac{1}{1 - i\omega\tau} + i\frac{n_s e^2}{m^* \omega}, \qquad (1)$$

where we assume the Drude-like normal fluid, e is the electric charge, and n_n/m^* and n_s/m^* are the normal fluid and the superfluid density over the effective mass, respectively. At low

temperatures and at low frequencies, the assumption $\sigma_1 \ll \sigma_2$ is valid, and one obtains the relation

$$X_s = \mu_0 \omega \lambda_L, \tag{2}$$

where λ_L is the London penetration depth. Since λ_L is related to n_s via the London equation $\lambda_L^{-2} = \mu_0 n_s e^2/m^*$, $\lambda_L(T)$ at low temperatures will give us information about the superconducting gap structure, particularly the presence or the absence of nodes in the gap.

Figure 1 shows the temperature dependence of Z_s at the three frequencies. In general, R_s increases as the frequency increases. However, in our samples, crystal 3 at 44 GHz measurement shows the lowest R_s at 1.6 K. This result indicates that the main contribution to the residual surface resistance $R_s^{\rm res}$ has an extrinsic origin. The surface impedance measurements are susceptible to defects on the sample surface. For layered conductors in general, the presence of delaminated edges on the sample is reported to cause excess loss of microwave power.[17] Thus we expect the thicker samples to show larger values of $R_s^{\rm res}$. In fact, crystal 3, which was cleaved from 2 after the 12 and 19 GHz measurements, is the thinnest among the samples and has the lowest $R_s^{\rm res}$, which agrees with the above expectation.

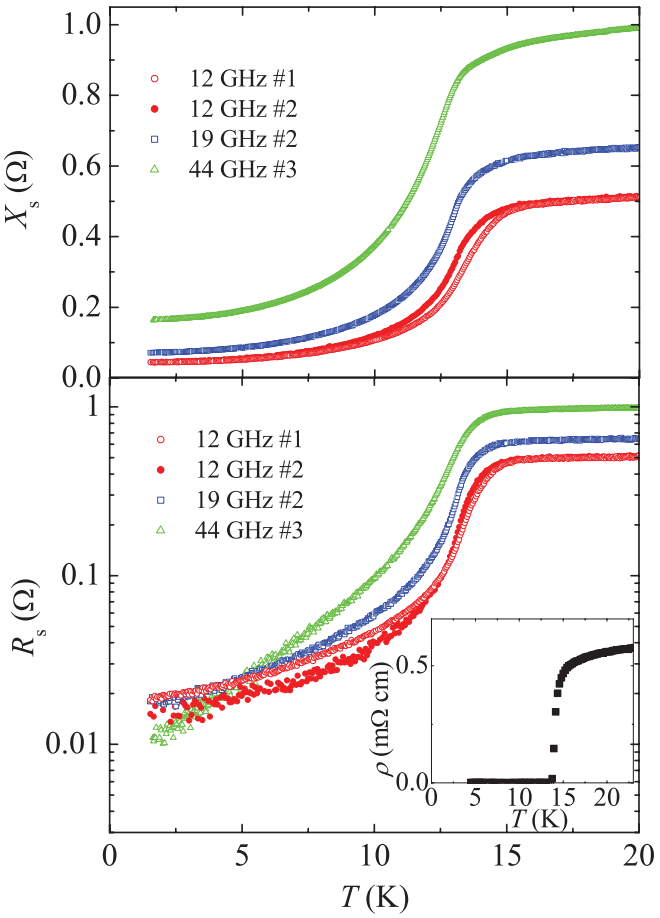

FIG. 1. (Color online) Temperature dependence of the microwave surface impedance of $FeSe_{0.4}Te_{0.6}$ single crystals, $Z_s = R_s - iX_s$, at 12, 19, and 44 GHz, respectively. All samples were from the same batch. Crystal 1 (with dimensions $1.0 \times 1.0 \times 0.1$ mm^3, $T_c = 14$ K) shows a sharper superconducting transition than crystal 2 ($0.7 \times 0.5 \times 0.1$ mm^3 for 12 and 19 GHz, $T_c = 13.5$ K) and crystal 3 ($0.5 \times 0.3 \times 0.05$ mm^3 for 44 GHz, $T_c = 13.5$ K). The inset shows $\rho(T)$ near T_c measured before cutting into small pieces for cavity measurements.

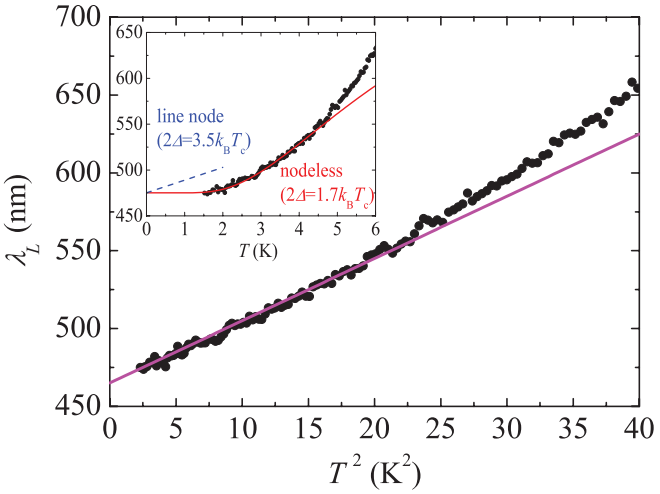

FIG. 2. (Color online) Temperature dependence of the magnetic penetration depth λ_L. The purple solid line represents the T^2 behavior. The inset shows the fit to nodeless s wave (red solid line) and the behavior of d wave with lines of nodes (blue dashed line).

Figure 2 shows $\lambda_L(T)$ for crystal 2 at low temperatures. The absolute value of λ_L at 0 K is $\lambda_L(0) \simeq 470$ nm, which is in fair agreement with the other measurements.[12,18] The penetration depth is found to behave in a power-law manner, $\delta\lambda_L \equiv \lambda_L(T) - \lambda_L(0) \propto CT^n$, with the exponent $n \simeq 2$. This behavior is also consistent with the previous electrodynamic study in the MHz region.[12,18] In general, a power-law temperature dependence implies the presence of low-energy quasiparticle excitations. In this case, the quasiparticle density of states (DOS) behaves as $D(E) \propto E^n$ close to the Fermi level, where E is the quasiparticle energy. At first sight, our result might seems to be inconsistent with a very flat DOS observed in an scannind tunneling microscopy (STM) study.[19] However, impurity scattering can cause quadratic temperature dependence. It has been shown that, in a two-band superconductor with $s_\pm$-wave symmetry with nonmagnetic impurities, the behavior of λ_L at low temperature is essentially the same as in a conventional s-wave superconductor with a considerable amount of magnetic impurities.[20] However, our samples might contain both magnetic and nonmagnetic impurities. Thus we cannot determine whether sign change exists or not from this experiment.

Figure 3(a) shows $\sigma_1(T)$ in the superconducting state. By subtracting $R_s^{\rm res}$ from the raw data of R_s before calculating σ, we can avoid the influence of surface defects and precisely discuss the quasiparticle dynamics. It should be noted that a small error in estimating $R_s^{\rm res}$ does not change the essential feature of $\sigma_1(T)$ at large. In all samples, a considerable enhancement of σ_1 was observed below T_c. Although the magnitude of the peak is somewhat different between the two samples (see the 12 GHz data), it tends to decrease with increasing frequency. It is well known that in the clean limit of the BCS superconductors, $\sigma_1(T)$ has a coherence peak. However, the peaks observed in our $\sigma_1(T)$ data are

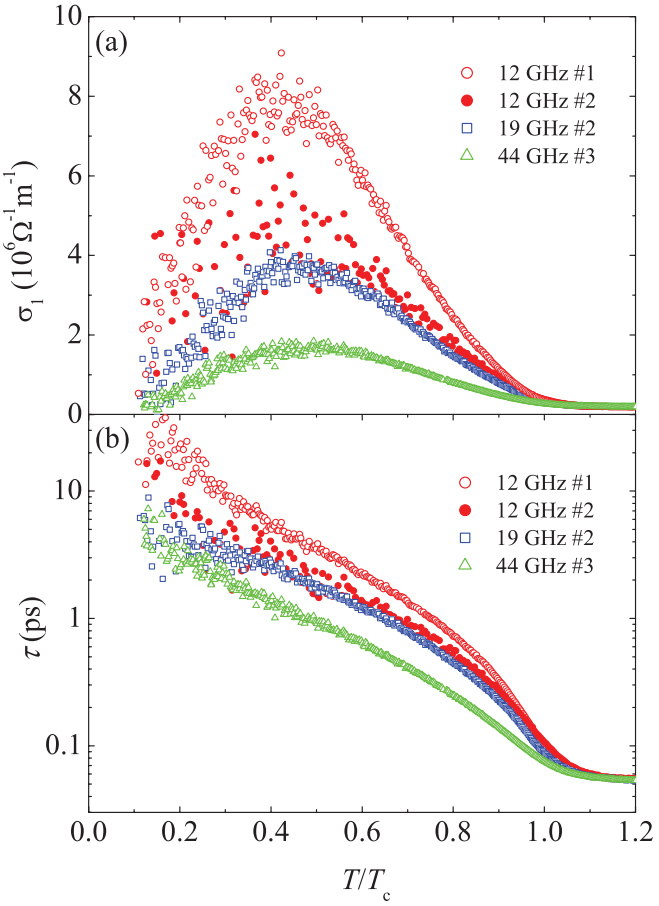

FIG. 3. (Color online) (a) Temperature dependence of the real part of the microwave conductivity. (b) The temperature dependence of the quasiparticle scattering time in the superconducting state.

much larger and broader than the coherence peak. Such peaks were also observed in the cuprate superconductors[21–23] and in other iron-based superconductors.[6,7] Below T_c, quasiparticle scattering is suppressed because the quasiparticle DOS near the Fermi level decreases by the emergence of the superconducting gap, giving rise to the peak in $\sigma_1(T)$ below T_c.

Since the coherence effect is not important in this system, we used the two-fluid model [see Eq. (1)] to extract τ and n_s as follows:

$$\omega\tau = \frac{\tilde{\sigma_1}}{1-\tilde{\sigma_2}}, \tag{3}$$

$$\frac{n_s(T)}{n_s(0)} = \tilde{\sigma}_2 - \frac{\tilde{\sigma}_1^2}{1-\tilde{\sigma}_2}, \tag{4}$$

where we assume that all carriers condense at $T = 0$ K. We also introduced the dimensionless conductivity $\tilde{\sigma} = \tilde{\sigma_1} + i\tilde{\sigma_2} = \mu_0\omega\lambda_L^2(0)(\sigma_1 + i\sigma_2)$. Figure 3(b) shows the temperature dependences of τ. As anticipated, we found the rapid increase in τ in all samples below T_c. The magnitude of the peak in $\sigma_1(T)$ reflects the degree of impurity scattering. In crystal 1, which has a larger peak than 2, τ increases more rapidly than in 2. The quasiparticle scattering time τ in crystal 1 reaches more than 10 ps far below T_c. This value is two orders of magnitude larger than that in the normal state and is comparable to that in LiFeAs in the superconducting state.[24]

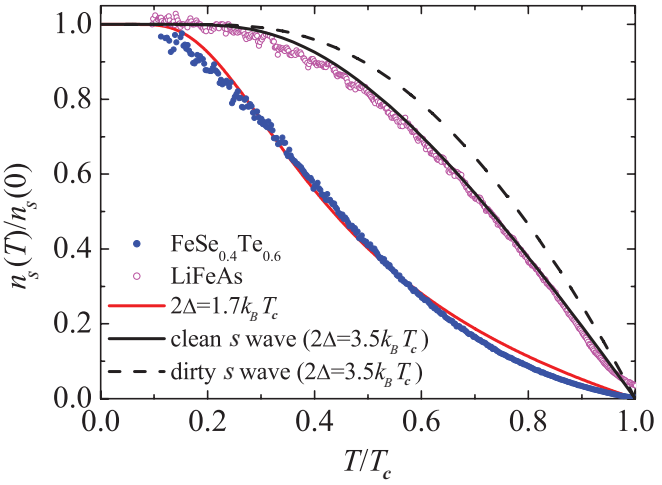

FIG. 4. (Color online) Temperature dependences of the superfluid density n_s in $FeSe_{0.4}Te_{0.6}$ and LiFeAs.[24] For clarity, only the 19 GHz data for crystal 2 are shown. The black solid (dashed) line is a curve expected for a conventional superconductor with $2\Delta = 3.5k_BT_c$ in the clean (dirty) limit. The red solid curve is a fit to clean s wave from $0.3T_c$ to T_c.

We find that τ depends on frequency. As frequency decreases, τ increases more rapidly in the superconducting state. Although we do not completely understand the origin of this frequency dependence, it might be related to the energy dependence of the DOS near the Fermi level. It is consistent with the observation that the frequency dependence is more profound at higher temperatures, where the number of thermally excited quasiparticles increases.

Next, we discuss $n_s(T)$. When Eq. (2) is valid, $n_s(T)$ is given by $n_s(T)/n_s(0) = \lambda_L(0)^2/\lambda_L(T)^2 = X_s(0)^2/X_s(T)^2$. However, there was some deviation from Eq. (2) at the highest measurement frequency, 44 GHz, and in the temperature range of 6–14 K, since the normal fluid contribution to X_s is not negligible. In this case, we have to consider the quasiparticle dynamics by analyzing σ data using Eq. (4). Figure 4 shows $n_s(T)/n_s(0)$ in crystal 2, which is very much different from that of the BCS superconductors. It is clear that this is convex downward in a wide temperature range. Near T_c, n_s increases very slowly with decreasing temperature, but this is irrelevant to the sample inhomogeneity such as the spatial distribution of Se content, because our samples show a rather sharp superconducting transition. In addition, damaged edges have almost no effect on $n_s(T)$.[25] For the conventional s-wave superconductors, such temperature dependence does not appear whether they are in the clean limit or the dirty limit.[26] This behavior is sometimes interpreted as a characteristic of multigap superconductors having at least one very small gap. If we try to fit the data by a two-gap model, where $n_s(T) = xn_{s1}(T) + (1-x)n_{s2}(T)$ $(0 < x < 1)$, we get the gap value $2\Delta \simeq 1.7\,k_BT_c$ for both gaps, which is much smaller than the value $2\Delta = 3.6\,k_BT_c$ clearly measured by STM.[19] This discrepancy indicates that the fitting using a simple two-gap model does not work for $FeSe_{0.4}Te_{0.6}$.

To explain this peculiar temperature dependence, we have to clarify whether $FeSe_{0.4}Te_{0.6}$ is a clean superconductor or not by comparing the electric mean free path l with the

coherence length ξ. We can calculate $l = v_F\tau$ with the Fermi velocity v_F measured by the angle-resolved photoemission spectroscopy (ARPES) on $FeSe_{0.5}Te_{0.5}$.[27] In ARPES, a very small v_F is observed for the outer hole pocket (α_3) centered at the Γ point and the electron pocket at the M point. With $v_F \simeq 1.4 \times 10^{-4}$ m/s for the α_3 pocket, l is about 7 Å just above T_c. This is half of the coherence length, $\xi \sim 15$ Å, estimated from an upper critical field measurement.[18,28] Thus the sample is in the dirty regime near T_c. As the temperature decreases, l extends with the rapid increase in τ, and $l >$ 100 Å at $0.5T_c$, which shows that the sample is in the clean limit.

Therefore, the behavior of $n_s(T)/n_s(0)$ can be understood as follows: only a small amount of quasiparticle collapses into the condensate near T_c because $l \simeq \xi$. At sufficiently low temperatures, the sample enters the clean limit, where n_s increases with a massive loss of conductivity spectral weight, resulting in an $n_s(T)/n_s(0)$ with a positive curvature. To summarize, it is important for $n_s(T)/n_s(0)$ in $FeSe_{0.4}Te_{0.6}$ that there is a crossover from the dirty regime to the clean regime in the superconducting state, with decreasing temperature. This interpretation can be applied also to other iron-based superconductors, such as the doped compounds $Ba(Fe,Co)_2As_2$[29] and $(Ba,K)Fe_2As_2$,[7] where similar temperature dependence is often observed. Furthermore, the report on $(Ba,K)Fe_2As_2$, which showed that $n_s(T)$ changes dramatically with a small impurity concentration,[7] can be understood as a result of the increase of ξ/l near T_c. On the other hand, as for the stoichiometric LiFeAs, which shows $\xi/l < 1$ even above T_c, $n_s(T)$ can be fitted by a simple two-gap model[24] because the samples are in the clean regime at all temperatures below T_c. For more quantitative analysis, we need to consider the multiband nature. For example, extending the two-gap model beyond the clean limit will reveal the value of superconducting gaps.

In conclusion, we have measured Z_s of $FeSe_{0.4}Te_{0.6}$ single crystals. The quadratic temperature dependence of λ_L indicates the presence of impurity scattering. In the superconducting state, an enhancement of σ_1 caused by the rapid increase of τ was observed. The temperature dependence of superfluid density $n_s(T)/n_s(0)$ shows a positive curvature in most of the temperature regime measured because the crystals are not in the clean limit near T_c and only become clean below T_c. This behavior indicates that one should carefully assess the relation between l and ξ in discussing $n_s(T)$ in iron-based superconductors.

We appreciate Noriyuki Nakai and Tetsuo Hanaguri for fruitful discussions.

[1] Y. Kamihara, T. Watanabe, M. Hirano, and H. Hosono, J. Am. Chem. Soc. **130**, 3296 (2008).
[2] J. Paglione and R. L. Greene, Nature Phys. **6**, 645 (2010), and references cited therein.
[3] I. I. Mazin, D. J. Singh, M. D. Johannes, and M. H. Du, Phys. Rev. Lett. **101**, 057003 (2008).
[4] K. Kuroki, S. Onari, R. Arita, H. Usui, Y. Tanaka, H. Kontani, and H. Aoki, Phys. Rev. Lett. **101**, 087004 (2008).
[5] H. Kontani and S. Onari, Phys. Rev. Lett. **104**, 157001 (2010).
[6] K. Hashimoto, T. Shibauchi, T. Kato, K. Ikada, R. Okazaki, H. Shishido, M. Ishikado, H. Kito, A. Iyo, H. Eisaki, S. Shamoto, and Y. Matsuda, Phys. Rev. Lett. **102**, 017002 (2009).
[7] K. Hashimoto, T. Shibauchi, S. Kasahara, K. Ikada, S. Tonegawa, T. Kato, R. Okazaki, C. J. van der Beek, M. Konczykowski, H. Takeya, K. Hirata, T. Terashima, and Y. Matsuda, Phys. Rev. Lett. **102**, 207001 (2009).
[8] J. D. Fletcher, A. Serafin, L. Malone, J. G. Analytis, J. H. Chu, A. S. Erickson, I. R. Fisher, and A. Carrington, Phys. Rev. Lett. **102**, 147001 (2009).
[9] J. K. Dong, S. Y. Zhou, T. Y. Guan, H. Zhang, Y. F. Dai, X. Qui, X. F. Wang, Y. He, X. H. Chen, and S. Y. Li, Phys. Rev. Lett. **104**, 087005 (2010).
[10] M. H. Fang, H. M. Pham, B. Qian, T. J. Liu, E. K. Vehstedt, Y. Liu, L. Spinu, and Z. Q. Mao, Phys. Rev. B **78**, 224503 (2008).
[11] A. Subedi, L. Zhang, D. J. Singh, and M. H. Du, Phys. Rev. B **78**, 134514 (2008).
[12] H. Kim, C. Martin, R. T. Gordon, M. A. Tanatar, J. Hu, B. Qian, Z. Q. Mao, Rongwei Hu, C. Petrovic, N. Salovich, R. Giannetta, and R. Prozorov, Phys. Rev. B **81**, 180503(R) (2010).
[13] B. C. Sales, A. S. Sefat, M. A. McGuire, R. Y. Jin, D. Mandrus, and Y. Mozharivskyj, Phys. Rev. B **79**, 094521 (2009).
[14] T. Taen, Y. Tsuchiya, Y. Nakajima, and T. Tamegai, Phys. Rev. B **80**, 092502 (2009).
[15] T. Noji, T. Suzuki, H. Abe, T. Adachi, M. Kato and Y. Koike, J. Phys. Soc. Jpn. **79**, 084711 (2010).
[16] T. J. Liu, X. Ke, B. Qian, J. Hu, D. Fobes, E. K. Vehstedt, H. Pham, J. H. Yang, M. H. Fang, L. Spinu, P. Schiffer, Y. Liu, and Z. Q. Mao, Phys. Rev. B **80**, 174509 (2009).
[17] J. S. Bobowski, J. C. Baglo, James Day, P. Dosanjh, Rinat Ofer, B. J. Ramshaw, Ruixing Liang, D. A. Bonn, and W. N. Hardy, Huiqian Luo, Zhao-Sheng Wang, Lei Fang, and Hai-Hu Wen, Phys. Rev. B **82**, 094520 (2010).
[18] T. Klein, D. Braithwaite, A. Demuer, W. Knafo, G. Lapertot, C. Marcenat, P. Rodière, I. Sheikin, P. Strobel, A. Sulpice, and P. Toulemonde, Phys. Rev. B **82**, 184506 (2010).
[19] T. Hanaguri, S. Niitaka, K. Kuroki, and H. Takagi, Science **328**, 474 (2010).
[20] A. B. Vorontsov, M. G. Vavilov, and A. V. Chubukov, Phys. Rev. B **79**, 140507(R) (2009).
[21] D. A. Bonn, P. Dosanjh, R. Liang, and W. N. Hardy, Phys. Rev. Lett. **68**, 2390 (1992).
[22] T. Shibauchi, A. Maeda, H. Kitano, T. Honda, and K. Uchinokura, Physica C **203**, 315 (1992).
[23] A. Hosseini, R. Harris, S. Kamal, P. Dosanjh, J. Preston, R. Liang, W. N. Hardy, and D. A. Bonn, Phys. Rev. B **60**, 1349 (1999).
[24] Y. Imai, H. Takahashi, K. Kitagawa, K. Matsubayashi, N. Nakai, Y. Nagai, Y. Uwatoko, M. Machida, and A. Maeda, J. Phys. Soc. Jpn. **80**, 013704 (2011).
[25] K. Cho, H. Kim, M. A. Tanatar, J. Hu, B. Qian, Z. Q. Mao, and R. Prozorov, e-print arXiv:1107.0711.

[26]M. Tinkham, *Introduction to Superconductivity*, 2nd ed. (Dover, New York, 1996), Chap. 3.

[27]A. Tamai, A. Y. Ganin, E. Rozbicki, J. Bacsa, W. Meevasana, P. D. C. King, M. Caffio, R. Schaub, S. Margadonna, K. Prassides, M. J. Rosseinsky, and F. Baumberger, Phys. Rev. Lett. **104**, 097002 (2010).

[28]Y. Imai, R. Tanaka, T. Akiike, M. Hanawa, I. Tsukada, and A. Maeda, Jpn. J. Appl. Phys. **49**, 023101 (2010).

[29]R. T. Gordon, Gordon, N. Ni, C. Martin, M. A. Tanatar, M. D. Vannette, H. Kim, G. D. Samolyuk, J. Schmalian, S. Nandi, A. Kreyssig, A. I. Goldman, J. Q. Yan, S. L. Bud'ko, P. C. Canfield, and R. Prozorov, Phys. Rev. Lett. **102**, 127004 (2009).